

Level-Crossing Studies of Na<sub>2</sub> Using Laser-Induced Fluorescence\*

M. McCLINTOCK

National Bureau of Standards and Department of Physics and Astrophysics, University of Colorado, Boulder, Colorado 80302

AND

W. DEMTRÖDER† AND R. N. ZARE‡

Joint Institute for Laboratory Astrophysics, University of Colorado, Boulder, Colorado 80302

(Received 18 April 1969)

The technique of using laser excitation to study level crossings in molecules has been developed and used to determine the radiative lifetime of an excited state of Na<sub>2</sub>. Optical detection of level crossing in the  $v'=10$ ,  $J'=12$  level of the  $B^1\Pi_u$  electronic state of Na<sub>2</sub>, excited by the 4765-Å argon-ion laser line, has resulted in a precise measurement of the product  $g\tau=4.11\pm 0.12\times 10^{-11}$  sec, corresponding to a magnetic field half-width of  $1385\pm 42$  G. If the  $g$  value is calculated assuming Hund's coupling case (a), the radiative lifetime is determined to be  $\tau=6.41\pm 0.38\times 10^{-9}$  sec. The influence of molecular hyperfine structure on this measurement is discussed and is found in general to contribute little uncertainty to the value of the radiative lifetime, provided the rotational angular momentum is much larger than the nuclear spin and/or provided the hyperfine interaction is much smaller than the natural width of the excited state.

## I. INTRODUCTION

Throughout the history of atomic spectroscopy, the study of the Zeeman effect has provided an exceedingly powerful tool for elucidating the nature of the atom and its interaction with radiation.<sup>1</sup> For example, among other things, the Zeeman effect has (1) laid the physical basis for the space quantization of angular momentum, (2) provided evidence through the anomalous Zeeman effect together with multiplet spectra for the spin of the electron, and (3) furnished information on nuclear spin and nuclear structure through the behavior of atomic hyperfine levels in a magnetic field. By contrast, the study of the effect of magnetic fields on the spectra emitted by molecules has not played a central role in the understanding of molecular structure, but rather has come to be regarded by many as a specialized technique of limited application.<sup>2</sup>

Why is the Zeeman effect so much more useful for atoms than molecules? It is clear that the magnetic separation of energy levels of both atoms and molecules is due to the same fundamental cause. Namely, in each case we have in a classical formulation a mechanical gyroscope possessing a magnetic moment; when an external magnetic field is applied to this mechanical

system, it exerts a torque on the magnetic moment, which tends to align it along the field direction. However, the gyroscopic forces present cause the magnetic moment to precess about the magnetic field direction at the Larmor frequency.

Let  $\mathbf{J}$  denote the total mechanical angular momentum of the system and let  $M$  be the projection of  $\mathbf{J}$  upon the field  $\mathbf{H}$ . In the presence of an external magnetic field the magnetic sublevels split apart, and their separate energies are given by the scalar product of the magnetic moment  $\boldsymbol{\mu}$  with the magnetic field  $\mathbf{H}$ :

$$E = -\langle \boldsymbol{\mu} \cdot \mathbf{H} \rangle \quad (1)$$

averaged over the state  $J, M$ . In general,  $\boldsymbol{\mu}$  is not along  $\mathbf{J}$  but moves around as the system rotates and therefore has some average projection along  $\mathbf{J}$ . If the Larmor frequency of precession is small compared to the frequency associated with the rotation of  $\boldsymbol{\mu}$  around  $\mathbf{J}$ , then we have

$$\begin{aligned} E &= \langle [(\boldsymbol{\mu} \cdot \mathbf{J})/\mathbf{J}] \cdot [(\mathbf{J} \cdot \mathbf{H})/\mathbf{J}] \rangle \\ &= \left[ \frac{\text{average magnetic moment along } \mathbf{J}}{\text{total angular momentum}} \right] \mu_0 M H, \end{aligned} \quad (2)$$

where  $\mathbf{J}$  is to be measured in units of  $\hbar$ , and the magnetic moment is in units of the Bohr magneton,  $\mu_0=1.3997$  MHz/G. In Eq. (2) the expression in brackets is called the  $g$  factor or  $g$  value of the system.

The magnetic moment  $\boldsymbol{\mu}$  has about the same magnitude for atoms and molecules since it depends on the spin and orbital angular momentum of the electrons in much the same way in both cases. However, in the case of a molecule,  $\boldsymbol{\mu}$  is often directed along the internuclear axis, whereas the direction of  $\mathbf{J}$  is determined primarily by the rotation of the much heavier nuclei. Since  $\boldsymbol{\mu}$  and  $\mathbf{J}$  are nearly perpendicular to each other, the value of  $g$  is much reduced from that of an atom. Moreover, the number of magnetic sublevels is propor-

\* This cooperative project was supported by National Science Foundation Grant GP-8095, National Institute of Health Grant GM-11123-04, and by the Advanced Research Projects Agency of the Department of Defense monitored by Army Research Office—Durham under Contract DA-31-124-ARO-D-139.

† JILA :Visiting Fellow, 1967–1968. Present address: Physikalisches Institut der Universität, Freiberg, Germany.

‡ Alfred P. Sloan Fellow. Present address: Chemistry Department, Columbia University, New York.

<sup>1</sup> E. U. Condon and G. H. Shortley, *The Theory of Atomic Spectra* (Cambridge University Press, New York, 1935). J. C. Slater, *Quantum Theory of Atomic Structure* (McGraw-Hill Book Co., New York, 1960), Vols. 1 and 2.

<sup>2</sup> For a review of the molecular Zeeman effect see F. H. Crawford, *Rev. Mod. Phys.* **6**, 90 (1934). For more recent work see C. H. Townes and A. L. Schawlow, *Microwave Spectroscopy* (McGraw-Hill Book Co., New York, 1955). N. F. Ramsey, *Molecular Beams* (The Clarendon Press, Oxford, 1956). D. W. Davies, *The Theory of the Electric and Magnetic Properties of Molecules* (John Wiley & Sons, Inc., New York, 1967).

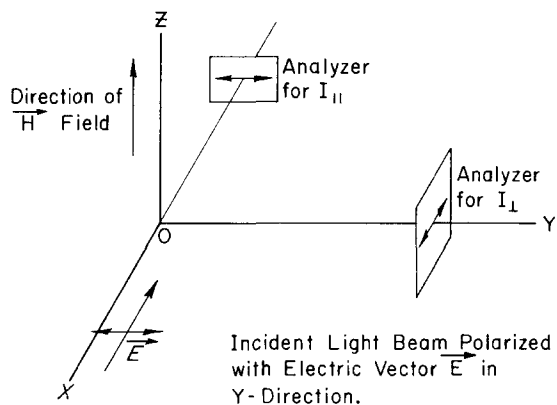


FIG. 1. Idealized experimental setup for studying the polarization of molecular fluorescence and its change with magnetic field. The light is incident along the  $X$  axis, and the molecular sample is located at the origin,  $O$ .

tional to  $2J+1$ . Hence, in the Zeeman pattern for a diatomic molecule we are normally confronted with a multiplicity of levels and a smallness of splitting that has no counterpart in atomic spectra. It should be no surprise then that even with the use of the highest dispersion spectrographs and the largest magnetic fields readily obtainable, the Zeeman splittings of most molecules appear to be incompletely resolved. The molecular Zeeman effect has therefore fallen into disuse in traditional optical spectroscopy.<sup>3</sup>

With the advent of microwave, ESR, and molecular beam resonance studies, a number of strikingly successful investigations have clearly shown the rich potentialities of the Zeeman effect in unraveling the intricate dynamics of internal molecular motions. These studies have been confined almost exclusively to ground-state species, but are also being extended to metastable states.<sup>4</sup> However, the study of short-lived excited states by these means appears to be impractical because of the low concentrations of such species which can be achieved.

Recently, it has been suggested that the difficulty of observing the effect of magnetic fields on excited molecular states can be overcome by level-crossing spectroscopy,<sup>5</sup> a technique long used in studies of atomic systems.<sup>6</sup> In this procedure, the change in the spatial distribution and polarization of the radiation re-emitted by excited molecules is observed in the presence of a variable external magnetic field. With a suitable choice of excitation and detection geometry the magnetic-field dependence of the fluorescent signal can be selected to have either a pure Lorentzian or a dispersion-shaped profile whose width is a measure of the product of the

$g$  value and the radiative lifetime  $\tau$  of the excited state of the molecule. If  $\tau$  is known from other measurements, the value of the  $g$  factor is determined from the level-crossing linewidth; alternatively, if  $g$  can be calculated from knowledge of the angular momentum coupling scheme in the molecule, the level-crossing linewidth then yields the value of the radiative lifetime. Although the optical detection of level crossings is an indirect measure of the Zeeman effect in molecules, the technique has the advantage that its resolution is not limited by the Doppler width of the molecular lines, as in conventional optical spectroscopy, but rather it can detect energy level changes at optical frequencies which are a fraction of the natural width of the molecular line.

The level-crossing phenomenon can be explained easily by referring to the idealized geometrical arrangement pictured in Fig. 1. Here a beam of plane-polarized resonance radiation is incident along the  $X$  axis with its electric vector  $\mathbf{E}$  pointing along the  $Y$  axis. The fluorescence sample is located at the origin  $O$ , and an external magnetic field may be applied along the  $Z$  axis. Fluorescence detectors are placed along the  $Y$  axis to measure the intensity,  $I_{\perp}$ , of light plane polarized along the  $X$  axis, and also along the  $X$  axis to measure the intensity,  $I_{\parallel}$ , of light plane polarized in the same direction as the incident light beam. In the absence of an externally applied field (zero field), the Zeeman levels of the excited molecular state are "crossed," i.e., degenerate within their natural width. If these levels are excited by the unidirectional beam of polarized light shown in Fig. 1, the molecular levels will be coherently excited and the phase relations between the Zeeman levels will cause interference terms which alter the angular distribution of the resonance fluorescence while preserving the resonance fluorescent rate. The anisotropy is traditionally measured by the *degree of polarization*, defined as

$$P = (I_{\parallel} - I_{\perp}) / (I_{\parallel} + I_{\perp}). \quad (3)$$

In general, the molecular fluorescence is observed to have a degree of polarization roughly the same as the exciting beam. However, if a magnetic field is applied, the Zeeman levels are "uncrossed," their coherence is partially destroyed, and the resonance fluorescence is depolarized.

Classically we may picture the excitation of the molecule by polarized light as causing oscillation of an elastically bound electron in the direction of  $\mathbf{E}$ , i.e., along the  $Y$  axis of Fig. 1. At zero magnetic field the excitation decays with a time constant equal to the radiative lifetime, but the oscillating electron always points along its initial direction. This results in a dipole radiation pattern with the fluorescence being polarized as well as spatially anisotropic. Suppose a magnetic field  $\mathbf{H}$  is now applied along the  $Z$  axis. The elastically bound electron then executes Larmor precession about  $\mathbf{H}$  in the  $X$ - $Y$  plane, and as a consequence, the fluorescence becomes less polarized and more isotropic. There is then a competition between the precession rate and

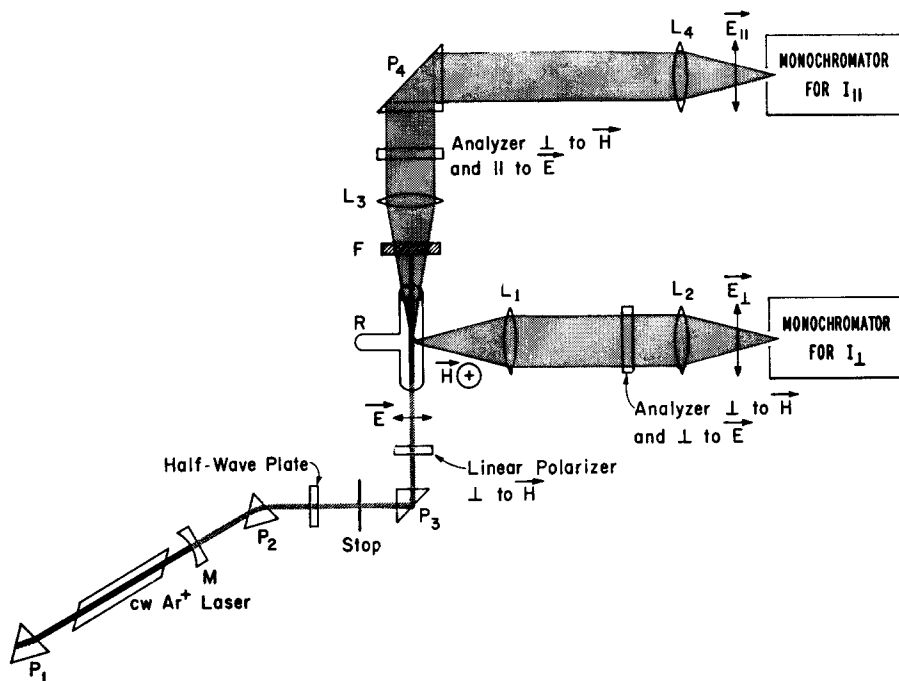
<sup>3</sup> G. Herzberg, *Spectra of Diatomic Molecules* (D. Van Nostrand Co., Inc., Princeton, N.J., 1950).

<sup>4</sup> See A. Carrington, D. H. Levy, and T. A. Miller, *J. Chem. Phys.* **47**, 3801 (1967) and references therein.

<sup>5</sup> R. N. Zare, *J. Chem. Phys.* **45**, 4510 (1966).

<sup>6</sup> For a review see B. Budick, in *Advances in Atomic and Molecular Physics*, D. R. Bates and I. Estermann, Eds. (Academic Press Inc., New York, 1967), Vol. 3, pp. 73-117.

FIG. 2. Schematic arrangement of the equipment used in the laser-induced molecular level-crossing experiment: M = mirror, L = lens, P = prism, F = filter, and R = reservoir. The magnetic field is perpendicular to the plane of the figure.



the radiation rate to determine the degree of polarization and the anisotropy of the fluorescence. More detailed considerations show that the field dependence of the polarization for the arrangement shown in Fig. 1 has the Lorentzian form

$$P(H) = P(0) \{1 + [(2g\tau\mu_0 H)/\hbar]^2\}^{-1}, \quad (4)$$

where  $P(0)$  is the degree of polarization at zero field. Thus, from a measurement of the polarization of the fluorescence as a function of magnetic field the product  $g\tau$  can be determined.

The first successful applications of level-crossing studies to molecules have been reported for NO,<sup>7</sup> CS,<sup>8</sup> and OH.<sup>9</sup> In these investigations molecular excitation is achieved using strong atomic lines or molecular lines of the same species produced in a discharge. In the preceding paper,<sup>10</sup> hereafter referred to as I, we describe the selective excitation of  $(v', J')$  levels of the Na<sub>2</sub> molecule using the cw lines of an argon-ion laser. From a study of the molecular resonance fluorescence, improved spectroscopic constants are reported in I for both the excited and ground states of this molecule, from which potential curves and Franck-Condon factors are calculated. In the present paper we report on the use of laser-induced fluorescence as a means of observing

molecular level crossings. In particular, the 4765-Å laser line has been used to determine the product  $g\tau$  for the  $v' = 10, J' = 12$  level of the  $B^1\Pi_u$  electronic state of the Na<sub>2</sub> molecule. In developing a technique for using laser excitation in molecular level-crossing studies we hope to increase significantly the number of molecular species which can be studied, not only by making the observation of level crossings in normally weak spectra possible, but also by enabling us to use the large number of laser wavelengths presently available or likely to become available for potential molecular excitation.

We shall first describe the experimental arrangement which permits the determination of  $g\tau$ . Since the radiative lifetime of the Na<sub>2</sub> molecule is so short and the  $g$  value so small [ $g = 1/J'(J'+1)$ ], large magnetic fields are required to observe the level crossing. This causes the additional complication that the overlap between the laser line and the Na<sub>2</sub> absorption line changes with magnetic field. However, we find that this bothersome Zeeman scanning effect can be eliminated by simultaneously measuring the level-crossing signal with two detectors placed at different angles to the excitation beam. A careful discussion of systematic sources of errors is included. Following the experimental discussion, the theory of molecular level crossings in a  $^1\Pi$  electronic state with and without hyperfine structure is presented, from which the value of the radiative lifetime is deduced based on the calculated molecular  $g$  value.

## II. EXPERIMENTAL

A block diagram of the equipment used for the present level-crossing study is shown in Fig. 2. The geometrical arrangement closely parallels the setup illustrated in

<sup>7</sup> D. R. Crosley and R. N. Zare, Phys. Rev. Letters **18**, 942 (1967); Bull. Am. Phys. Soc. **12**, 1147 (1967); J. Chem. Phys. **49**, 4231 (1968).

<sup>8</sup> S. J. Silvers, T. H. Bergeman, and W. Klemperer, 23rd Symposium on Molecular Structure and Spectroscopy, Ohio State University, Columbus, Ohio, September 1968.

<sup>9</sup> A. Marshall, R. L. deZafra, and H. Metcalf, Phys. Rev. Letters **22**, 445 (1969); Bull. Am. Phys. Soc. **14**, 620 (1969). K. R. German and R. N. Zare, "Measurement of the Hanle Effect for the OH Radical," Phys. Rev. (to be published).

<sup>10</sup> W. Demtröder, M. McClintock, and R. N. Zare, J. Chem. Phys. **51**, 5495 (1969) this issue.

Fig. 1. The 4765-Å beam from a cw argon-ion laser is passed through a half-wave plate which rotates the plane of polarization so that  $\mathbf{E}$  is brought perpendicular to  $\mathbf{H}$  without sacrifice of power. A linear polarizer is placed before the alkali cell to ensure that the incident light is linearly polarized with its electric vector  $\mathbf{E}$  at right angles to the magnetic field  $\mathbf{H}$  (which is directed perpendicular to the plane of Fig. 2). A 5-Å-wide region of the Na<sub>2</sub> fluorescence spectrum, centered at 5339.6 Å is then observed in two directions, parallel to the incident beam and at right angles to the beam. Under excitation by the 4765-Å laser line, this region of the Na<sub>2</sub> fluorescence spectrum corresponds to a pair of *P* and *R* lines ( $v' = 10, J' = 12$ )  $\rightarrow$  ( $v'' = 19, J'' = 12 \pm 1$ ) which appear at 5338.649 Å (vac) and 5340.573 Å (vac), respectively. Analyzers are placed in the detection optics by the monochromators shown in Fig. 2 to ensure observation of light polarized with its electric vector parallel,  $I_{||}$ , and perpendicular,  $I_{\perp}$ , to  $\mathbf{E}$ . The dc signals from the photomultipliers of each monochromator are amplified, processed arithmetically as described below, and recorded as a function of magnetic field. Note that in most level-crossing experiments the magnetic field dependence of the intensity is monitored, whereas here we record the change in the degree of polarization with magnetic field.

To observe the level-crossing effect, we require only a source of excitation, a supply of molecules, a magnetic field and a means of detecting the fluorescent light. We will discuss each of these requirements in turn.

### A. Experimental Apparatus

An ideal level-crossing light source should supply an intense, stable beam of resonance radiation. Although the intensity of the laser beam far exceeds conventional light sources, it is inherently unstable due to the vagaries of the discharge conditions. However, the stability requirements are, in general, modest; for our detection system they are sufficiently relaxed that laser excitation provides a very powerful and useful light source for level-crossing studies.

The argon-ion laser is a water-cooled carbon-disc design having an auxiliary magnet which produces a field of approximately 1000 G axial to the 60 cm by 2.5 mm bore. With an internal prism,  $P_1$ , for wavelength selection and an output mirror,  $M$ , of 94% reflectivity at 4880 Å, the output power is about 1 W at either 4880 Å or 5145 Å, and 150 mW at 4765 Å, when a current of 15 A flows through the laser discharge bore. The laser power is measured with a silicon calorimeter calibrated against a National Bureau of Standards calorimeter.<sup>11</sup> A prism,  $P_2$ , is used to further disperse the beam and remove uv plasma lines. A third prism,  $P_3$ , directs the beam through the Na<sub>2</sub> fluorescence cell.

The argon-ion laser is operated multimode; the laser line typically consists of one or two Doppler components, depending on the operating parameters, each of which is composed of many spectrally narrow cavity resonances (modes). The width of the one or two Doppler gain curves is typically about 2 GHz and the spacing between adjacent modes is about 0.06 GHz so that many different modes are oscillating simultaneously, the number depending on the current, magnetic field, pressure, etc. These modes change in wavelength at frequencies typically of the order of kilocycles, so that the effective radiation has a characteristic spectral distribution given by the Doppler gain curve.

The construction of the Na<sub>2</sub> fluorescence cell is similar to that described in I, with the exception that the cell's heater is wound in a bifilar manner with molybdenum wire. At first, nichrome wire was used, as in I, but the large magnetoresistance of nichrome makes this unsatisfactory because it introduces spurious magnetic-field-dependent effects. Molybdenum wire, with its much-lower magnetoresistance, was therefore used instead. The dimensions of the cell were chosen to accommodate the gap of the magnet. The cell was filled by distilling sodium into it and sealing it off while the system was under a vacuum of  $10^{-6}$  torr.

Both reservoir and cell temperatures were measured with thermocouples in contact with the outer surface of the glass. The thermocouple voltages were read with a potentiometer to  $\pm 2 \mu\text{V}$  ( $0.05^\circ\text{C}$ ), although the temperature gradients across the cell are expected to be somewhat larger. The thermocouples were calibrated against a glass-mercury thermometer of  $0.05^\circ\text{C}$  accuracy by placing the oven and thermocouple assembly in a large laboratory drying oven. The oven surrounding the cell was made of copper to promote temperature uniformity.

The electromagnet used to produce the field at the fluorescence cell had conical pole pieces tapered to 3.2-cm diam. At a separation of 2.5 cm, a maximum of approximately 15 kG could be obtained. The field was determined to be uniform to within  $\frac{1}{2}\%$  over the central 2.5 cm of the pole pieces. The detection optics were carefully adjusted to collect radiation from within this volume. The strength of the magnetic field was measured with a Hall probe and dc amplifier which had an analog output.<sup>12</sup>

The molecular fluorescence was dispersed with two scanning monochromators (Ebert mount with 1200-line/mm grating) placed at right angles to each other as shown in Fig. 2. A photomultiplier tube was mounted on the exit slit of each monochromator, each shielded against stray magnetic field changes with a housing material of high magnetic permeability. The change of sensitivity of each photomultiplier as a function of the fringing magnetic field from the electromagnet was measured by illuminating the entrance slit of each

<sup>11</sup> D. A. Jennings, K. M. Evenson, W. R. Simmons, and A. I. Rasmussen, Conference on Laser Measurements, Warsaw, Poland, September 1968.

<sup>12</sup> Model 120 gaussmeter, Bell Inc., Columbus, Ohio.

monochromator with an incandescent lamp operated from a current-regulated power supply. In addition, small corrections for the scattered light background and the photomultiplier dark current were made in taking data.

Initially we used only one detector to monitor the change of  $I_{\perp}$  with increasing magnetic field. However, this conventional experimental configuration produced non-Lorentzian level-crossing signals which were a source of much consternation. It soon became apparent that the change in  $I_{\perp}$  with increasing magnetic field was caused not only by the anticipated level-crossing effect but also by the change in the absorption of the laser excitation as the magnetic sublevels of the excited state move apart. This latter effect is a serious problem which will occur whenever level crossings are observed in molecular excited levels with large  $J$ , small  $g$  and short  $\tau$ . To overcome this magnetic scanning of the molecular absorption profile with respect to the laser profile, two detectors are used in a bidirectional manner as discussed below.

### B. Corrections for Magnetic-Field-Dependent Absorption

Most theoretical treatments of the level-crossing effect assume broad-band excitation where the power density of the lamp radiation is uniform across the Doppler profile of the absorbers.<sup>13</sup> The effect of departure from a flat lamp profile has been examined by Gallagher and Lurio.<sup>14</sup> It was shown that the shape of the level-crossing curve is altered in a manner which can be evaluated theoretically in terms of the power density of the lamp at each frequency, integrated over the absorption frequency of the scatterers. This correction to atomic level-crossing studies seldom exceeds 1% and its consideration is often neglected.<sup>15</sup>

Recently, Series<sup>16</sup> has considered the case of excitation by a monochromatic light beam where the spectral width is small compared to the natural width. Such excitation corresponds to the spectral character of a single laser mode. His analysis indicates that "the important variable is the spectral distribution of the exciting light as seen by the atoms in relation to the natural width of the excited levels" from which he concludes that "level-crossing curves excited by monochromatic light should be identical with those by broad-band excitation, provided the Doppler width for absorption in the vapor is large compared with the natural width."

In the case of Na<sub>2</sub> the Doppler width is some 40 times the natural width (based on the radiative lifetime determined in this paper), and it might appear at first glance that no complications would result from the use of the multimode laser line as an excitation source.

This conclusion would be incorrect, however, for it disregards the fact that molecular excitation often involves upper state levels with very large total angular momentum ( $J \gtrsim 10$ ) compared to the atomic case. These large angular momentum states cause extensive broadening of the absorption profile. When the magnetic sublevels are each separated by the natural width, the absorption profile is then broadened by  $(2J+1)$  times the natural width. Thus, for the  $v'=10, J'=12$  level of the  $B^1\Pi_u$  state of Na<sub>2</sub> the separation between the extreme components,  $M'=J'$  and  $M'=-J'$  of the line is comparable to the Doppler width, even though the natural width of this level is much smaller. Consequently, it follows for this level (and molecular levels like this) that a magnetic field strong enough to produce considerable depolarization of the fluorescence will also be strong enough to cause the fluorescence intensity to change with field due to the Zeeman scanning of the  $M$ -state components of the absorption line over the complex profile of the laser excitation.

A theoretical calculation of the correction for this effect would require knowledge of the convolution of the absorption profile with the laser profile as a function of magnetic field.<sup>14</sup> We do not have sufficient information on the complex line structure of the laser beam to make this approach workable. Instead, we have chosen to follow an experimental procedure which separates the magnetic-field-dependent absorption from the level-crossing signal. This procedure is based on measuring the change of polarization with magnetic field using the bidirectional detection system<sup>17</sup> shown in Fig. 2. Zeeman scanning of the absorption profile causes the level-crossing signal,  $I(H)$ , for both parallel and perpendicular observation directions to be multiplied by a magnetic-field-dependent factor,  $f(H)$ . The observed fluorescence signals,  $S(H)$ , are then related to the level-crossing signal  $I(H)$  by

$$S_{\parallel}(H) = I_{\parallel}(H)f(H) \quad (5a)$$

and

$$S_{\perp}(H) = KI_{\perp}(H)f(H) \quad (5b)$$

for the two detector directions. The constant  $K$  has been inserted in Eq. (5b) to allow for differences in the sensitivity of the optics and electronics for the two observation directions. The degree of polarization [See Eqs. (3) and (4)] may then be expressed in terms of  $S(H)$  by

$$P(H) = P(0) [1 + (2g\tau\mu_0 H/\hbar)^2]^{-1} \\ = \frac{S_{\parallel}(H) - S_{\perp}(H)/K}{S_{\parallel}(H) + S_{\perp}(H)/K} \quad (6)$$

Equation (6) shows that by recording  $P(H)$  as a function of  $H$ , found from simultaneous measurements of  $S_{\parallel}(H)$  and  $S_{\perp}(H)$ , the product  $g\tau$  may then be determined, free from the effects of magnetic scanning.

<sup>13</sup> P. A. Franken, Phys. Rev. **121**, 508 (1961).

<sup>14</sup> A. Gallagher and A. Lurio, Phys. Rev. **136**, A87 (1964).

<sup>15</sup> W. W. Smith and A. Gallagher, Phys. Rev. **145**, 26 (1966).

<sup>16</sup> G. W. Series, Proc. Phys. Soc. (London) **89**, 1017 (1966).

<sup>17</sup> We thank Dr. K. B. Persson, National Bureau of Standards, Boulder, Colo., for kindly loaning us the additional spectrometer we used.

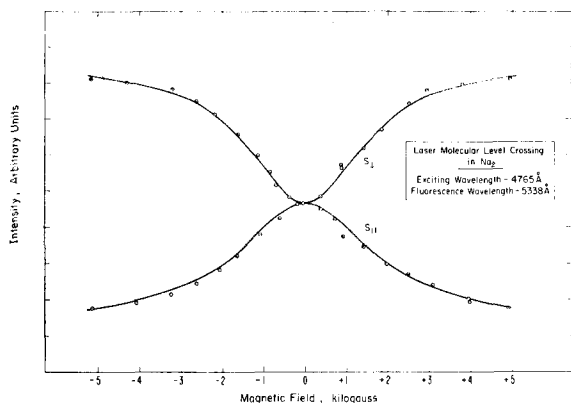


FIG. 3. Intensity data  $S_{\perp}$  and  $S_{\parallel}$ , separately recorded as a function of magnetic field. Solid curves represent the best least-squares fit of a Lorentzian curve to the data points. The half-widths of the two Lorentzians differ, illustrating the necessity for treating the experimental data as explained in the text.

The value of  $K$  may be set equal to unity by choosing the gain of the photomultiplier tubes so that the signals  $S_{\parallel}(H)$  and  $S_{\perp}(H)$  are equal in the limit of high magnetic field. However, in practice it is more convenient to adjust the value of  $K$  so that the two signals  $S_{\parallel}(H)$  and  $S_{\perp}(H)$  are equal at zero magnetic field,  $H=0$ , i.e.,

$$K = S_{\parallel}(0)/S_{\perp}(0) = [1+P(0)]/[1-P(0)]. \quad (7)$$

When this is done

$$P(H) = \frac{S_{\parallel}(H) - S_{\perp}(H)[1-P(0)]/[1+P(0)]}{S_{\parallel}(H) + S_{\perp}(H)[1-P(0)]/[1+P(0)]}. \quad (8)$$

The zero-field degree of polarization of the  $P$  and  $R$  lines resulting from a  $\Delta J = -1$  transition to the excited rotational level  $J'$  may be calculated from the average of the  $P$  and  $R$  branch polarizations<sup>5</sup>

$$P(0) = \frac{1}{2} \left[ \frac{1}{7} + (2J'^2 - J') / (14J'^2 + 33J' + 20) \right]. \quad (9)$$

For  $J' = 12$ ,  $P(0) = 0.128$  so that from Eq. (7),  $K = 0.773$ . The experimentally measured value for this quantity, obtained by taking the ratios of the intensities at zero-magnetic field, was  $K = 0.770$ , which gives us confidence in this experimental method of correcting for the magnetic-field-dependent absorption.

The complex structure of the laser line, both in the time and frequency domains, forces consideration of other related effects on the shape of the level-crossing curve. At any instant, the spectrum of the multimode laser is described by the convolution of the Doppler gain curve with the actual mode structure of the laser cavity. For some laser lines the Doppler gain curve is composed of not just one, but two Zeeman components,<sup>18</sup> depending on the laser current and magnetic field, which further complicates the structure. In addition to

<sup>18</sup> W. Demtröder and M. McClintock, "Antipolarized Spectral Lines from Inelastic Collisions of Laser-Excited Molecules" (unpublished).

this, mechanical instabilities in the laser cavity and instabilities in the plasma itself cause the cavity mode structure to vary with time under the gain curve (so-called mode hopping). The mechanical features of the laser cavity typically have resonances in the kilocycle to megacycle range, which is also the range of frequencies characteristic of plasma instabilities. Hence, the mode-hopping time is anticipated to be more than  $10^3$  times slower than the radiative lifetime of the molecule. However, the observation time is long compared with the mode-hopping time, so that the observed fluorescence is characteristic of the averaged effects of the convolution of the absorption profile with the laser line structure under the gain curve.

In order to experimentally test the effect of mode hopping on the form of the level-crossing curve, several laser parameters were varied in order to change the complex spectral and temporal character of the exciting radiation. First, the laser cavity was lengthened from 1.2 to 2 m. This nearly halves the spacing of the adjacent cavity modes from 0.002 to 0.00125  $\text{cm}^{-1}$ . The actual mode structure of the laser may be a multiple of this spacing. No change in the level-crossing curve was observed within 1%. Next, the laser current was reduced from 15 to 10 A. This results in both a lower output intensity and a narrower gain curve. Again, no effect on the level-crossing curve could be detected other than a small change attributable to stimulated emission, discussed later.

We have shown how to compensate experimentally for the lack of white-light excitation by recording the degree of polarization  $P(H)$  based on the difference and sum of  $I_{\parallel}(H)$  and  $I_{\perp}(H)$ . These arguments, taken with the experimental evidence obtained for the insensitivity of the level-crossing curve to the laser mode structure, indicate that the present technique, used properly, can lead to accurate measurements of molecular level crossings using laser lines as an excitation source.

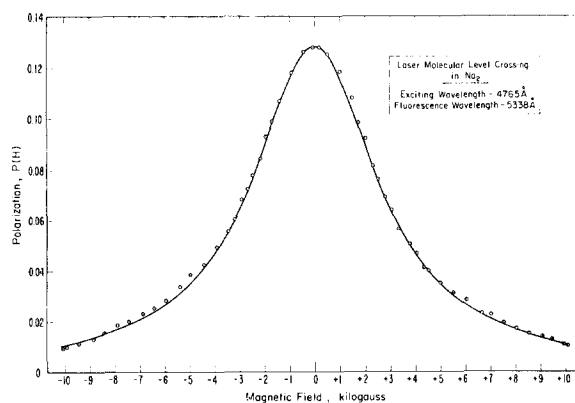


FIG. 4. The degree of polarization,  $P(H)$ , of the resonance fluorescence resulting from the  $v' = 10$ ,  $J' = 12 \rightarrow v'' = 3$ ,  $J'' = 11$ , 13 transitions plotted as a function of the magnetic field,  $H$ . The curve through the experimental points is the Lorentzian curve that fits the data best in a least-squares sense.

### C. Results and Error Discussion

Figure 3 shows a record of the two functions  $S_{||}(H)$  and  $KS_{\perp}(H)$  for fluorescence from the  $v'=10, J'=12$  excited level of the Na<sub>2</sub> B<sup>1</sup>Π<sub>u</sub> state detected in the manner described. Although each function is approximately Lorentzian, curves were observed resulting from fluorescence from higher rotational levels of the excited state for which marked deviations were observed due to the magnetic scanning of the Zeeman levels of the molecule.

Figure 4 gives the experimental points, calculated according to Eq. (8), for the level-crossing signal. It should be stressed that Fig. 4 illustrates the change with magnetic field of the degree of polarization, rather than of the intensity, as is more commonly the case in level-crossing experiments. A Lorentzian curve calculated from a least-squares fit is drawn through the data points.

When the detection system departs<sup>19</sup> from the ideal geometry shown in Fig. 1 with respect to the central angle of the optics or to the analyzer angles, the level-crossing curve is not, in general, symmetric about  $H=0$ . A record of both sides of the level-crossing curve provides a convenient check on the alignment of the experimental setup, although this is redundant if the excitation and detection geometry is known to be sufficiently close to ideal. The painstaking care used in aligning the experimental geometry, the polarizers and the analyzers apparently was justified as can be seen from the right-left symmetry about  $H=0$  of the curve shown in Fig. 4. This alignment was greatly facilitated by the use of laser excitation. After proper alignment, all data recorded were symmetric about  $H$  to about  $\pm 1\%$ , and this figure was further improved by averaging both sides of the level-crossing curve. In this manner level-crossing half-widths were determined under various experimental conditions.

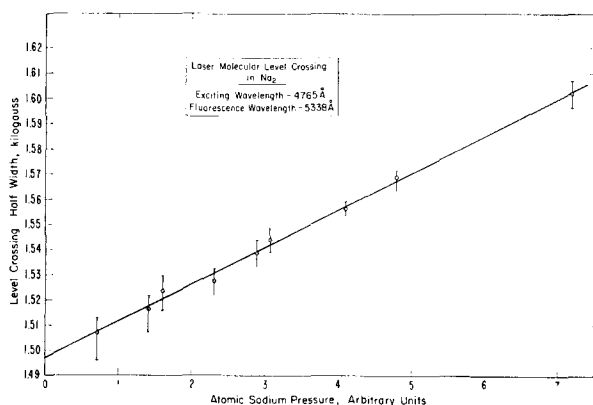


FIG. 5. Plot of measured  $H_{1/2}$  versus atomic sodium pressure. The magnetic field at the center of the pole gap was  $7.6\% \pm 0.2\%$  lower than that measured at the pole face. Thus the zero pressure intercept is found to be  $1385 \pm 42$  G.

<sup>19</sup> A. Lurio and R. Novick, *Phys. Rev.* **134**, A608 (1964); A. Lurio, R. L. deZafra, and R. J. Goshen, *ibid.* **134**, A1198 (1964).

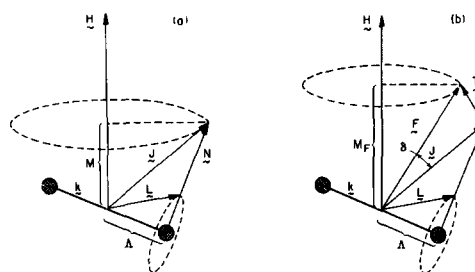


FIG. 6. Vector model for the coupling of angular momenta in a <sup>1</sup>I<sub>1</sub> electronic state: (a) without nuclear-spin coupling, (b) with nuclear-spin coupling.

The shape of the level-crossing curve depends on the density of the scatterers in two ways: (1) by multiple scattering of the fluorescence radiation<sup>20</sup> and (2) by collisional effects.<sup>21-24</sup> For molecules, in general, radiation trapping is seldom a significant correction due to the large number of branching transitions from the excited ( $v', J'$ ) level to all the ( $v'', J''$ ) levels of the ground state, most of which are not thermally populated. On the other hand, the effects of several different kinds of collisions must be considered in the case of molecular level-crossing spectroscopy. An inelastic collision that occurs while the molecule is in the excited ( $v', J'$ ) level causes the apparent lifetime of that state to be shortened, and hence broadens the level-crossing curve. However, while electronic quenching collisions and depolarization collisions clearly operate to broaden the level-crossing curve in this way, collisions which change the rotational and/or vibrational levels can have other effects. Such collisions can populate nearby levels which produce spectral lines that lie within a few  $\text{cm}^{-1}$  of the fluorescence lines under observation. In general, the polarization characteristics and magnetic-field dependence are different from those of the original lines. If the lines originating from collisionally populated states lie within the pass band of the detection system, their effect on the level-crossing curve must be carefully considered.

Fortunately, the effects of collisional broadening and multiple scattering on the level-crossing curve may be eliminated experimentally by extrapolating to zero pressure. Figure 5 shows the half-width at half-maximum of the Lorentzian curve which best fits the level-crossing data at each reservoir temperature plotted against the pressure of atomic sodium that corresponds to the reservoir temperature. The smoothed vapor pressure compilation of Nesmeyanov<sup>25</sup> is used to determine the pressure-temperature relationship. The extrapolated

<sup>20</sup> J. P. Barrat, *J. Phys. Radium* **20**, 633, 657 (1959).

<sup>21</sup> F. W. Byron and H. M. Foley, *Phys. Rev.* **134**, A625 (1964).

<sup>22</sup> A. Omont, *J. Phys. Radium* **26**, 26 (1965).

<sup>23</sup> M. I. D'Yakonov and V. I. Perel, *Zh. Espk. Teor. Fiz.* **48**, 345 (1965) [*Sov. Phys.—JETP* **21**, 227 (1965)].

<sup>24</sup> W. Happer and E. B. Saloman, *Phys. Rev. Letters* **15**, 441 (1965).

<sup>25</sup> A. N. Nesmeyanov, *Vapour Pressure of the Elements* (Academic Press Inc., New York, 1963).

value of the half-width,  $H_{1/2} = 1385$  G, is estimated to be accurate to  $\pm 3\%$ .

The slope of the curve shown in Fig. 5 contains information about the cross section for the destruction of alignment in the ( $v' = 10, J' = 12$ ) state by the collisional processes of electronic quenching, depolarization, etc. However, no attempt has been made to analyze this data for such information due to the likely presence of foreign gas in the cell at higher temperatures.

In addition to extrapolating the data to zero pressure, it is necessary to extrapolate to zero laser intensity because the intensity of the incident radiation in the focus of a powerful laser beam is great enough to cause a shortening of the radiative lifetime by stimulated emission, which is proportional to the laser power density.<sup>26</sup> The half-width of the level-crossing curve was plotted against the average incident power and the half-width was found to decrease slightly as the laser power decreases. The slope of the line through the measured half-widths contains information on the cross section for stimulated emission. However, the evaluation of the cross section would require knowledge of the laser-beam power-density profile and this point was not pursued further.

Another potential source of error is the possibility of unequal populations of the ground-state magnetic sublevels (optical pumping) resulting from the high incident power of the laser beam.<sup>27</sup> We have observed departures from the theoretical value of the degree of polarization at zero field at high laser intensities which may be attributed to this effect. The circulation of coherence between the ground and excited states and its effect on level-crossing measurements has been considered by Baylis.<sup>28</sup> He shows that optical pumping will not alter the shape of the level-crossing curve, provided the magnetic sublevels of the excited state are split apart in an equally spaced pattern, as is the case for  $\text{Na}_2$ . In any case an extrapolation to zero laser power, which we have performed, will eliminate any possible errors from this cause or from stimulated emission.

The estimated accuracy of  $\pm 3\%$  contains several factors. The first is the precision which is easily calculated from a least-squares fit of a Lorentzian curve to the data. For any given level-crossing curve, the scatter typically leads to a standard deviation of  $\pm \frac{1}{2}\%$ . This figure represents predominantly the effect of noise caused by fluctuations in the laser intensity and by dark current in the photomultiplier tubes. The method of taking data, however, eliminated much of the effect of these fluctuations. An RC filter with a 2-sec time constant was used in the output circuit of each of the dc amplifiers that received the photomultiplier tube signals. Each of the points on the level-crossing curve was

recorded by noting the sum or the difference intensity at a given value of magnetic field minus the intensity at zero field. Each observation was integrated over approximately 4 sec after elimination of the initial transient of approximately 6 sec. In essence, this amounts to phase-sensitive detection at a frequency of 3 cycle/min (standard graduate-student chopping frequency), so that random noise of any higher frequency was effectively eliminated. The precision of  $\pm \frac{1}{2}\%$  is presented as evidence for the efficiency of noise elimination by this detection method.

Even noise of lower frequency than 3 cycle/min is partly eliminated by this method of recording, although not so efficiently. Here we assume that these effects are linear over the time required to make an observation at a given magnetic field between two observations at zero field, and then we correct the central observation by interpolation of the drift between zero-field readings. Drift of the laser intensity or of the amplifiers is as likely to be positive as negative, as shown by a separate observation of their characteristics. Therefore these drifts tend to be eliminated by this method of recording. However, temperature changes of the oven caused by a change of the electrical resistance of the heater windings in a magnetic field (magnetoresistance) always produce a change of the same sign in the observed intensity. Specifically, this causes a spurious broadening of the level-crossing curve. We have mentioned that this magnetoresistive effect was minimized by using molybdenum heater wire. In addition, the data points were taken in such a sequence that the average field applied was a constant; high-field and low-field points were alternated. The thermal time constant of the oven was approximately 100 times that of the time required for a measurement, and thus helped to reduce the magnetoresistive effect. An estimate of the error in the width of the level-crossing curve was made by noting the change in oven temperature as a function of time after application of a fixed magnetic field and by relating this to the change in molecular density through the vapor pressure data. Using this method we estimate that magnetoresistance contributes approximately 0.2% uncertainty to  $H_{1/2}$  under our experimental conditions.

The Hall probe was mounted on one water-cooled magnet pole face. The magnetic-field strength at the center of the gap was  $7.6 \pm 0.2\%$  lower than the value measured by the probe. The probe also received some heat from the adjacent oven. The change in sensitivity was noted by establishing a value of magnetic field and noting the change in the Hall probe reading as the oven's temperature was raised. Under the most unfavorable conditions, a correction of  $+0.6\%$  in the magnetic field was necessary for this effect. Corrections were made for these systematic errors. More serious was the uncertainty caused by drift of the Hall probe amplifier. This was approximately  $\pm 1\frac{1}{2}\%$  at 3000 G after allowing the equipment to warm up properly (about  $\frac{1}{2}$  h). The Hall probe was calibrated against permanent magnets

<sup>26</sup> M. Dumont and B. Decomps, *J. Phys. Radium* **29**, 181 (1968); B. Decomps and M. Dumont, *ibid.* **29**, 443 (1968).

<sup>27</sup> R. E. Drullinger and R. N. Zare, *Bull. Am. Phys. Soc.* **14**, 486 (1969); "Optical Pumping of Molecules," *J. Chem. Phys.* (to be published).

<sup>28</sup> W. E. Baylis, *Phys. Letters* **26**, A414 (1968).



at 299 and 2970 G, which were themselves calibrated against an NMR probe. The over-all uncertainty in a measurement of magnetic field was estimated to be  $\pm 2\%$ .

Another possible source of systematic error is the lack of identical response of the dc photomultiplier amplifiers. With identical input signals, they agreed with each other to within  $\pm 0.2\%$ .

Other sources of error have been mentioned previously. Estimates of the uncertainty they contribute to  $H_{1/2}$  are listed here. Deviations from perfect alignment were found from the right-left asymmetry of the level-crossing curves to cause less than  $\pm 0.3\%$  uncertainty. Changes in sensitivity of the photomultiplier tubes with magnetic field were found to be approximately  $0.2\%$  at 10 kG, less at lower fields. This contributes an error of  $\pm 0.1\%$  in  $H_{1/2}$ . Corrections for scattered light background and dark current of the photomultiplier tubes had no measurable magnetic field dependence, and hence contributed negligible error.

The largest source of systematic error would appear to be the extrapolation to zero pressure of the level-crossing half-width. We estimate that the effect of residual gases in the cell on the accuracy of  $H_{1/2}$  gives a maximum error of  $+2\%$ . Figure 5 shows the extrapolation of  $H_{1/2}$  to zero pressure.

Taking all the errors into consideration, both the easily calculable random errors and estimates of the systematic errors, we have assigned an accuracy of  $\pm 3\%$  to the value of  $H_{1/2} = 1385$  G. This corresponds to a measurement of the product  $g\tau = 4.11 \pm 0.12 \times 10^{-11}$  sec. This accuracy is comparable to that quoted for most atomic level-crossing experiments, and illustrates that the study of level crossing in molecules by laser excitation, using the techniques described, can provide accurate information on the structure of molecular excited states.

### III. DISCUSSION OF RESULTS

The product  $g\tau$  for the ( $v' = 10, J' = 12$ ) positive  $\Lambda$ -doublet level of the Na<sub>2</sub>  $B^1\Pi_u$  electronic state has been determined directly from the change in the degree of polarization of the fluorescent light with magnetic field. To interpret this measurement we must carefully discuss the nature of the angular momentum coupling scheme in this excited state and determine how a change of coupling with magnetic field may affect the apparent  $g\tau$  product. The  $^1\Pi_u$  state follows<sup>2,3</sup> Hund's coupling case (a), i.e., the strongest interaction is between the molecular axis  $\mathbf{k}$  and the orbital angular momentum  $\mathbf{L}$  so that  $\mathbf{L}$  precesses about the molecular axis making a constant projection  $\Lambda$  on  $\mathbf{k}$ . For a  $^1\Pi$  state, the spin angular momentum is zero and the absolute value of  $\Lambda$  is one. The rotational angular momentum of the nuclei  $\mathbf{N}$  then adds vectorially to  $\Lambda\hat{\mathbf{k}}$  to form the resultant total angular momentum  $\mathbf{J}$ , excluding nuclear spin. A vector diagram of this coupling scheme for a  $^1\Pi$  electronic state is shown in Fig. 6(a). The behavior

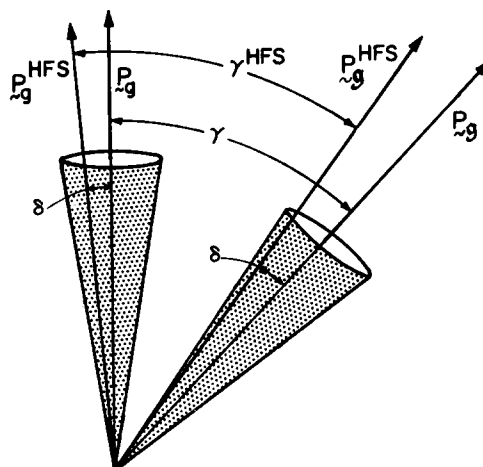


FIG. 7. Orientation of the absorption ( $P_g^{HFS}$ ,  $P_g$ ) and emission ( $P_g^HFS$ ,  $P_g$ ) dipole oscillators with and without hyperfine structure. This diagram shows the relationship between the various angles subtended. The angle  $\delta$  is the same as in Fig. 6(b).

of a  $^1\Pi$  electronic state (excluding nuclear spin) is that of a symmetric top. If a magnetic field is applied, the total angular momentum  $\mathbf{J}$  then precesses about  $\mathbf{H}$  making a projection  $M$  on the space-fixed magnetic-field direction, as illustrated in Fig. 6(a).

The Na<sup>23</sup> nucleus is a fermion having a nuclear spin of  $I = \frac{3}{2}$ . The total nuclear spin angular momentum  $\mathbf{T}$  of the Na<sub>2</sub> molecule has the values  $T = 3, 2, 1$ , and  $0$ . For such a homonuclear molecule, however, symmetric states always occur with even  $T$  values and antisymmetric states with odd  $T$  values. Consequently, we need only consider the values of  $T = 3$  and  $1$  for the positive (antisymmetrical)  $\Lambda$  doublet populated by the ( $v'' = 3, J'' = 13$ )  $\rightarrow$  ( $v' = 10, J' = 12$ ) transition. In molecular states with electronic angular momentum, magnetic hyperfine structure is usually comparable in size with magnetic hyperfine structure in atoms<sup>2,3</sup> and is usually much larger than that due to electric quadrupole moments. It is expected that  $\mathbf{T}$  and  $\mathbf{J}$  couple together to form the resultant  $\mathbf{F}$ , as shown in Fig. 6(b). If a magnetic field is then applied,  $\mathbf{F}$  precesses about  $\mathbf{H}$  with a projection upon  $\mathbf{H}$  of  $M_F$ , provided the field strength is not sufficient to uncouple  $\mathbf{T}$  from  $\mathbf{J}$ .

The behavior of the Na<sub>2</sub>  $B^1\Pi_u$  state in a magnetic field thus depends on the size of the interaction between the nuclear spin and the other molecular angular momenta compared to the interaction of the various angular momenta and the applied magnetic field. Although various hyperfine structure parameters are known for the Na<sub>2</sub>  $X^1\Sigma_g^+$  ground state,<sup>29</sup> there has

<sup>29</sup> The nuclear magnetic moment of <sup>23</sup>Na has been found by P. Kusch, S. Millman, and I. I. Rabi, Phys. Rev. **55**, 1176 (1939) to be  $\mu = 2.216$  nuclear magnetons. The sign and magnitude of the quadrupole interaction energy of the <sup>23</sup>Na nucleus in the <sup>23</sup>Na<sub>2</sub> molecule has been determined by R. A. Logan, R. E. Coté, and P. Kusch, *ibid.* **86**, 280 (1952), to be  $eqQ/h = -0.423$  MHz. The gyromagnetic ratio  $g_J = \mu_J/J$ , where  $\mu_J$  is the rotational magnetic moment and  $J$  is the rotational angular momentum, has been measured by R. A. Brooks, C. H. Anderson, and N. F. Ramsey, *ibid.* **136**, A62 (1968). They report  $g_J = 0.03892$  nuclear magnetons for the ground state Na<sub>2</sub> molecule.

TABLE I. Some nonvanishing direction cosine products averaged over all orientations. The direction cosine matrix element  $\Phi_{F'g}$  is the cosine of the angle between the space-fixed axes  $F=X, Y, Z$ , and the molecule-fixed axes  $g=x, y, z$ .

Direction cosine product <sup>a</sup>	Average value
$\Phi_{F'g}^4$	1/5
$\Phi_{F'g}^2\Phi_{F'g'}^2$	1/15
$\Phi_{F'g}^2\Phi_{F'g''}^2$	1/15
$\Phi_{F'g}^2\Phi_{F'g'}^2$	2/15
$\Phi_{F'g}\Phi_{F'g'}\Phi_{F'g''}\Phi_{F'g''}$	-1/30

<sup>a</sup> Here it is understood that  $F \neq F'$  and  $g \neq g'$ .

been no measurement of the hyperfine structure, etc., for the  $B^1\Pi_u$  excited state. To be strictly accurate we must formulate the quantum mechanical expectation values of the operators of interest.<sup>30</sup> However, for large  $J$ , the molecular system is nearly classical and we shall rely heavily on the vector models shown in Figs. 6(a) and 6(b) for estimating the effects of hyperfine interaction.

The interaction term we wish to evaluate is

$$H_{TL} = A\mathbf{T} \cdot \mathbf{L}. \quad (10)$$

According to the vector model we may rewrite (10) as

$$\begin{aligned} H_{TL} &= A\langle \mathbf{L} \cdot \hat{k} \rangle_{Av} \langle \hat{k} \cdot \mathbf{J} \rangle_{Av} \langle \hat{J} \cdot \mathbf{T} \rangle_{Av} \\ &= A\Lambda \{ \Lambda / [J(J+1)]^{1/2} \} \{ \mathbf{J} \cdot \mathbf{T} / [J(J+1)]^{1/2} \} \\ &= [A\Lambda^2 / J(J+1)]^{1/2} [F(F+1) - J(J+1) - T(T+1)]. \end{aligned} \quad (11)$$

From Eq. (11) it is apparent that the hyperfine interaction energy decreases with increasing rotational angular momentum. From the vector model [Fig. 6(b)] it is clear that as  $J$  increases it becomes more nearly perpendicular to the molecular axis  $\mathbf{k}$ . Moreover  $\mathbf{J}$  and  $\mathbf{F}$  become nearly parallel to each other and of equal length. Taken together, these effects physically cause the  $H_{TL}$  hyperfine interaction to rapidly diminish in magnitude with increasing  $J$ .

Then for some reasonable value of the hyperfine interaction constant,  $A$ , we would expect the interaction  $A\mathbf{T} \cdot \mathbf{L}$  for the  $J' = 12$  rotational level to be less than the coupling of  $\mathbf{J}$  to  $\mathbf{H}$  at the level-crossing half-width. Thus the  $B^1\Pi_u$  electronic state of the  $\text{Na}_2$  molecule might be expected to follow a coupling scheme as in Fig. 6(b) for zero field ( $H=0$ ) but to change over to the coupling scheme shown in Fig. 6(a) as the strength of the external field is increased. This would affect the apparent value of  $g\tau$  that we measure since both the  $g$  value and the degree of polarization depend on the angular momentum coupling scheme of the molecular excited state. Again we will use the results of simple vector model calculations to estimate the magnitude of these effects.

<sup>30</sup> R. A. Frosch and H. M. Foley, Phys. Rev. **88**, 1337 (1952).

### A. The Influence of hfs on the $g$ Value

The  $B^1\Pi_u$  electronic state of the  $\text{Na}_2$  molecule is paramagnetic and because of the large Zeeman effect associated with the electronic orbital angular momentum we may neglect the contributions to the magnetic moment from (1) the nuclear magnetic moments of the nuclei, (2) the rotational magnetic moment of the molecule and (3) the diamagnetism set up by currents opposing the applied field. The magnetic interaction energy is then given by<sup>31</sup>

$$H_{JH} = -\boldsymbol{\mu}_L \cdot \mathbf{H}, \quad (12)$$

where  $\boldsymbol{\mu}_L = -\mu_0\mathbf{L}$ . For the vector coupling scheme shown in Fig. 6(a)

$$\begin{aligned} H_{JH} &= \mu_0 \langle \mathbf{L} \cdot \hat{k} \rangle_{Av} \langle \hat{k} \cdot \hat{J} \rangle_{Av} \langle \hat{J} \cdot \mathbf{H} \rangle_{Av} \\ &= \mu_0 \Lambda \{ \Lambda / [J(J+1)]^{1/2} \} \{ \mathbf{J} \cdot \mathbf{H} / [J(J+1)]^{1/2} \} \\ &= [\Lambda^2 / J(J+1)] \mu_0 M H. \end{aligned} \quad (13)$$

From the definition for the  $g$  value given in Eq. (2) we obtain

$$g_J = [J(J+1)]^{-1}, \quad (14)$$

where  $\Lambda$  has been set equal to one for a  $\Pi$  state. The  $g$  value shown in Eq. (13) applies to any Hund's case (a)  $^1\Pi$  electronic state having no hyperfine structure or whose hyperfine structure is decoupled from  $\mathbf{J}$  (molecular Paschen-Back effect).<sup>2,3</sup>

For the vector coupling scheme shown in Fig. 6(b) in which the resultant nuclear spin  $\mathbf{T}$  is coupled to  $\mathbf{J}$ , the Zeeman energy is given by

$$\begin{aligned} H_{FH} &= \mu_0 \langle \mathbf{L} \cdot \hat{k} \rangle_{Av} \langle \hat{k} \cdot \hat{J} \rangle_{Av} \langle \hat{J} \cdot \hat{F} \rangle_{Av} \langle \hat{F} \cdot \mathbf{H} \rangle_{Av} \\ &= \mu_0 \Lambda \left( \frac{\Lambda}{[J(J+1)]^{1/2}} \right) \left( \frac{\mathbf{J} \cdot \mathbf{F}}{[J(J+1)F(F+1)]^{1/2}} \right) \\ &\quad \times \left( \frac{\mathbf{F} \cdot \mathbf{H}}{[F(F+1)]^{1/2}} \right) \\ &= \frac{\Lambda^2}{J(J+1)} \frac{F(F+1) + J(J+1) - T(T+1)}{2F(F+1)} \mu_0 M_F H. \end{aligned} \quad (15)$$

<sup>31</sup> At magnetic fields sufficient to observe level-crossing effects in  $\text{Na}_2$  it might be questioned whether the magnetic field strength would be large enough to disturb the end-over-end rotational motion of the molecule as well. This would distort the molecular wavefunctions due to the field, and the energy splitting may be estimated from second-order perturbation theory in a manner analogous to the quadratic Stark effect. For a  $^1\Pi$  electronic state we find

$$\begin{aligned} \Delta W &= \frac{(\Lambda\mu_0 H)^2}{2B_v} \left( \frac{(J-\Lambda^2)(J-M^2)}{J^2(2J-1)(2J+1)} \right. \\ &\quad \left. - \frac{[(J+1)^2 - \Lambda^2][(J+1)^2 - M^2]}{(J+1)^2(2J+1)(2J+3)} \right), \end{aligned}$$

where  $B_v$  is the molecular rotational constant of the  $v$ th vibrational level of the excited state. This second-order interaction energy alters the observed level-crossing signal by causing the magnetic sublevels to be unequally split in the field  $H$ . For the  $v'=10$ ,  $J'=12$  level of the  $\text{Na}_2 B^1\Pi_u$  state, however, this effect is negligible for fields on the order of  $H \approx 2000$  G, and thus may be neglected.

The  $g$  value for a <sup>3</sup>H state with hyperfine structure is thus

$$g_F = g_J \left( \frac{F(F+1) + J(J+1) - T(T+1)}{2F(F+1)} \right). \quad (16)$$

For a <sup>3</sup>H electronic state having no hyperfine structure or for which the hyperfine structure is small compared to the Zeeman energy, we expect the level-crossing curve to be a Lorentzian-shaped curve with a  $g$  value given by Eq. (14). Thus we would calculate  $g_{J'} = 0.006410$  for  $J' = 12$ . However, when hyperfine structure cannot be neglected, the result is many different  $g$  values, each one corresponding to a value of Eq. (16) for a particular pair of values  $F$  and  $T$ . The level-crossing curve is no longer a single Lorentzian, but a sum of Lorentzians. However, if the  $g_F$  values differ little from each other, as would be the case for the  $J' = 12$ ,  $T = 1$  or 3 level of Na<sub>2</sub>, the curve would be almost identical to a Lorentzian with a  $g$  value which is the average of the individual  $g$  values. If Eq. (16) is summed over all  $F$  and  $T$  values weighted by the product  $F(F+1) \cdot T(T+1)$  we obtain  $\langle g_F \rangle_{Av} = 0.006272$ . Thus the presence of hyperfine structure causes approximately a 2% smaller  $g$  value and consequently a 2% broader level-crossing curve. This would be an overestimate of the effect if the coupling scheme changes from Fig. 6(b) to Fig. 6(a) with increasing magnetic field. In this case the  $g$  value would be field dependent (molecular Breit-Rabi effect) and the level-crossing curve would be no longer strictly Lorentzian. Within our precision, however, we could not detect any systematic departure from a Lorentzian shape in the present case.

Note that in atomic level-crossing studies the presence of different isotopes of various nuclear spin greatly complicates analysis since the atomic  $g$  factor is so sensitive to the nature of the hyperfine coupling and the magnitude of the nuclear spin.<sup>1</sup> However, for molecules with  $|J| \gg |T|$  the above classical arguments show that the effect of hyperfine structure on the molecular  $g$  value is normally quite slight. From the vector model we see that this result is expected whenever  $\mathbf{J}$  and  $\mathbf{F}$  are nearly parallel and almost of equal length. For the excited level of Na<sub>2</sub> under study, if we assume that  $\mathbf{J}$  and  $\mathbf{T}$  couple together, we find the contribution from  $J' = 12$  does not totally eclipse that from  $T = 3$ , but the calculated change of the  $g$  value is nevertheless quite small.

## B. The Influence of hfs on the Degree of Polarization

The product  $g_T$  is determined from Eq. (4) based on the change in the degree of polarization  $P(H)$  of the fluorescent light as a function of the field  $H$ . However, if the coupling scheme in the excited state also changes with  $H$ , there will be another source for the variation of  $P(H)$  which has not been included in Eq. (4). To

TABLE II. Classical expressions for the square of the cosine of the angle,  $\cos^2\gamma^{hfs}$ , between the absorption and emission oscillators when hyperfine structure is present. The angle  $\delta$  is defined in Eq. (26). Note that as  $\delta$  approaches zero,  $\cos^2\gamma^{hfs}$  approaches  $\cos^2\gamma$ .

$\gamma$	$\cos^2\gamma$	$\cos^2\gamma^{hfs}$
0°	1	$\frac{1}{2}(1 - 2\cos^2\delta + 3\cos^4\delta)$
45°	$\frac{1}{2}$	$\frac{1}{8}(3 - 2\cos^2\delta + 3\cos^4\delta)$
90°	0	$\frac{1}{4}(1 + 2\cos^2\delta - 3\cos^4\delta)$

estimate the magnitude of this possible effect, we calculate the zero-field degree of polarization  $P(0)$  for the two different coupling cases shown in Fig. 6.

Let  $F = X, Y, Z$  refer to the laboratory space-fixed axes and  $g = x, y, z$  to the molecule-fixed axes. The direction cosine matrix elements  $\Phi_{Fg}$  then relate the two coordinate systems which have for their common origin the center of mass of the molecule.<sup>32</sup> We shall assume that we may describe the absorption and emission process classically where we replace the electric dipole transition moment of the molecule by a Hertzian dipole oscillator pointed in the same direction and attached rigidly to the molecular framework. Let the incident light be polarized along  $\mathbf{E}_F$  and let it excite an absorption oscillator along  $\mathbf{P}_g$ . The probability for excitation is then proportional to  $\Phi_{Fg}^2$ . Let the emission oscillator be along  $\mathbf{P}_g$ , where  $g$  does not necessarily coincide with  $g$ . The probability for emission with light polarized along  $\mathbf{E}_{F'}$  is proportional to  $\Phi_{F'g}^2$ . Thus for light emitted plane polarized in the same direction as the electric vector of the incident light we have

$$I_{||} \propto \langle \Phi_{Fg}^2 \Phi_{F'g}^2 \rangle_{Av} \quad (17)$$

and for light emitted plane polarized in a direction perpendicular to the electric vector of the incident light we have

$$I_{\perp} \propto \langle \Phi_{Fg}^2 \Phi_{F'g}^2 \rangle_{Av}, \quad (18)$$

where  $F' \neq F$ . The averages indicated in Eqs. (17) and (18) are over all initial orientations of the molecule.

The direction cosines  $\Phi_{Fg}$  and  $\Phi_{F'g}$  are related to each other by

$$\Phi_{F'g} = \sum_g \Phi_{F'g} \Phi_{Fg} \quad (19)$$

and thus

$$\Phi_{F'g}^2 = \sum_{g1} \sum_{g2} \Phi_{F'g1} \Phi_{F'g2} \Phi_{Fg1} \Phi_{Fg2}. \quad (20)$$

With the help of Eq. (20), Eqs. (17) and (18) can be rewritten as

$$I_{||} \propto \langle \sum_{g1} \sum_{g2} \Phi_{F'g1}^2 \Phi_{F'g2}^2 \Phi_{Fg1}^2 \Phi_{Fg2}^2 \rangle_{Av} \quad (21a)$$

<sup>32</sup> The direction cosine matrix elements  $\Phi_{Fg}(\alpha, \beta, \gamma)$  are listed in Table I of Ref. 5, where  $\alpha, \beta, \gamma$  are Euler angles relating the  $XYZ$  and  $xyz$  reference frames. Note that in the present paper the molecule-fixed  $z$  axis corresponds to the symmetry axis of the molecule considered as a symmetric top and not the internuclear axis of the molecule.

and

$$I_{\perp} \propto \langle \sum_{\theta_1} \sum_{\theta_2} \Phi_{F\theta_1}^2 \Phi_{F'\theta_1} \Phi_{F'\theta_2} \Phi_{\theta_1\theta_2} \Phi_{\theta_2\theta_1} \rangle_{av}. \quad (21b)$$

In Table I we have collected<sup>33</sup> the only types of non-vanishing terms encountered in the evaluation of Eq. (21). With the additional identity

$$\sum_{\theta_1} \Phi_{\theta_1\theta_1}^2 = \sum_{\theta_2} \Phi_{\theta_2\theta_2}^2 = 1 \quad (22)$$

we find

$$I_{||} = (2/15) \langle \Phi_{\theta\theta}^2 \rangle + (1/15) \quad (23a)$$

and

$$I_{\perp} = (2/15) - (1/15) \langle \Phi_{\theta\theta}^2 \rangle. \quad (23b)$$

The quantity  $\langle \Phi_{\theta\theta}^2 \rangle$  is an ensemble average of the square of the cosine of the angle included between  $\mathbf{P}_{\theta}$  and  $\mathbf{P}_{\theta}$

$$\langle \Phi_{\theta\theta}^2 \rangle = \cos^2 \gamma \quad (24)$$

and represents the transition dipole moment autocorrelation function.<sup>34</sup> From Eqs. (3), (23), and (24) the degree of polarization may be related to the average angle  $\gamma$  between the absorption and emission oscillators by

$$P = (3 \cos^2 \gamma - 1) / (\cos^2 \gamma + 3). \quad (25)$$

Equation (25) is a well-known formula in the theory of the polarization of complex molecules<sup>35</sup> and was derived in a different manner by Levshin<sup>36</sup> and by Perrin<sup>37</sup> many years ago. From Eq. (25) we may derive a number of familiar results concerning the polarization of diatomic fluorescence (based on the classical limit). For a  $Q$ -branch transition ( $Q \uparrow$ ,  $Q \downarrow$ ),<sup>38</sup> the absorption and emission oscillators coincide and are directed along the angular momentum vector  $\mathbf{J}$  of the molecule. Then  $\cos^2 \gamma = 1$  and  $P = \frac{1}{2}$ . For a  $P$ - or  $R$ -branch transition ( $P \uparrow$ ,  $R \downarrow$ ), ( $P \uparrow$ ,  $P \downarrow$ ), ( $R \uparrow$ ,  $P \downarrow$ ), or ( $R \uparrow$ ,  $R \downarrow$ ) the absorption and emission oscillators point along the molecular axis, which rotates in a plane perpendicular to  $\mathbf{J}$ . Then  $\mathbf{P}_{\theta}$  and  $\mathbf{P}_{\theta}$  are distributed uniformly about a circle and the average (acute) angle between them is  $45^\circ$ , so that  $\cos^2 \gamma = \frac{1}{2}$  and  $P = \frac{1}{7}$ . Finally, for a transition of the type ( $P \uparrow$ ,  $Q \downarrow$ ), ( $Q \uparrow$ ,  $P \downarrow$ ), ( $R \uparrow$ ,  $Q \downarrow$ ), or ( $Q \uparrow$ ,  $R \downarrow$ ) the absorption and emission oscillators are at right angles to each other,  $\cos^2 \gamma = 0$  and  $P = -\frac{1}{3}$ . These values of  $P$  are the same as those obtained previously<sup>5</sup> for the classical limit.

Let us now consider how Eq. (25) is modified when

<sup>33</sup> These results, in part, are those given by E. B. Wilson, Jr., J. C. Decius, and P. C. Cross, *Molecular Vibrations* (McGraw-Hill Book Co., New York, 1955), Appendix 4.

<sup>34</sup> R. Zwanzig, *Ann. Rev. Phys. Chem.* **16**, 67 (1965); B. J. Berne, J. P. Boon, and S. A. Rice, *J. Chem. Phys.* **45**, 1086 (1966); R. G. Gordon, *ibid.* **45**, 1643 (1966).

<sup>35</sup> P. P. Feofilov, *The Physical Basis of Polarized Emission* (Consultants Bureau Enterprises, Inc., New York, 1961).

<sup>36</sup> V. L. Levshin, *Z. Physik* **32**, 307 (1925).

<sup>37</sup> F. Perrin, *Ann. Phys. (Paris)* **12**, 169 (1929).

<sup>38</sup> The notation here is the same as in Ref. 5. The arrow pointing upwards ( $\uparrow$ ) refers to absorption and the arrow pointing downwards ( $\downarrow$ ) to emission. The branches  $R$ ,  $Q$ ,  $P$  correspond to  $J' - J'' = 1, 0$ , and  $-1$ , respectively.

hyperfine structure is present. The absorption and emission oscillators  $\mathbf{P}_{\theta}^{\text{hfs}}$  and  $\mathbf{P}_{\theta}^{\text{hfs}}$  are still described as above, relative to the angular momentum vector  $\mathbf{J}$ . However,  $\mathbf{J}$  is no longer fixed in space but precesses instead about  $\mathbf{F}$  making an angle  $\delta$  [see Fig. 6(b)], where

$$\begin{aligned} \cos \delta &= \hat{\mathbf{J}} \cdot \hat{\mathbf{F}} \\ &= \frac{F(F+1) + J(J+1) - T(T+1)}{2[J(J+1)F(F+1)]^{1/2}}. \end{aligned} \quad (26)$$

We assume the precession rate is very rapid compared to the radiative lifetime of the molecular excited state. As a result the absorption and emission oscillators may be considered to be uniformly distributed on the surface of a cone making an apex half-angle of  $\delta$  with the axis of the cone, which points in the direction the absorption and emission oscillators would have in the absence of hyperfine structure. This is shown in Fig. 7 for some angle  $\gamma$  which  $\mathbf{P}_{\theta}$  and  $\mathbf{P}_{\theta}$  would subtend without hyperfine structure. The angle  $\gamma^{\text{hfs}}$  subtended by  $\mathbf{P}_{\theta}^{\text{hfs}}$  and  $\mathbf{P}_{\theta}^{\text{hfs}}$  may then be related to the angle  $\gamma$  formed between  $\mathbf{P}_{\theta}$  and  $\mathbf{P}_{\theta}$  by

$$\cos^2 \gamma^{\text{hfs}} = P_2(\cos \delta) [\cos^2 \gamma P_2(\cos \delta) + \frac{1}{2} \sin^2 \delta] + \frac{1}{2} \sin^2 \delta, \quad (27)$$

where  $P_2(\cos \delta) = (3 \cos^2 \delta - 1)/2$ .

In Table II we have summarized the expressions obtained for  $\cos^2 \gamma^{\text{hfs}}$  in terms of  $\cos^2 \delta$  for the three values of  $\gamma$  encountered in diatomic molecules. We note that in each case the effect of hyperfine structure is to depolarize the fluorescence, i.e., to make  $P$  tend toward zero with increasing values of the angle  $\delta$ . However as  $|\mathbf{J}|$  becomes much larger than  $|\mathbf{T}|$ , the wobble angle  $\delta$  tends toward zero, and the effect of hyperfine structure on the degree of polarization disappears. For the  $J' = 12$ ,  $T = 1$  and 3 level of the  $\text{Na}_2$  molecule the degree of polarization should strictly be calculated using quantum formulas [see Eq. (9)]. However, we may use the above classical expressions to estimate the reduction of  $P$  due to hyperfine interaction. Whereas  $P$  would equal 0.14286 in the absence of hyperfine structure we find  $P$  would have the value 0.12693 for the coupling scheme shown in Fig. 6(b). This is a decrease of more than 10% in the value of  $P$  and represents a readily measurable effect. If the coupling scheme remained unchanged with increasing magnetic field, the determination of  $gr$  would be independent of the value of  $P(0)$ . However, if the nuclear spin  $\mathbf{T}$  becomes uncoupled from the angular momentum  $\mathbf{J}$  with increasing magnetic field, the variation of  $P(H)$  with  $H$  would not be Lorentzian and the product  $gr$  would be in error. We may conclude then that as long as the coupling scheme is not itself field dependent, the influence of hyperfine structure on the product  $gr$  would be quite small. The results we have derived here concerning the effect of nuclear spin on the degree of polarization are quite general and show that for many molecular systems  $P$  is nearly unchanged by hyperfine interaction provided  $|\mathbf{J}| \gg |\mathbf{T}|$ .

### C. The Radiative Lifetime

We are aware of one earlier measurement of the Na<sub>2</sub> B <sup>1</sup>Π<sub>u</sub> radiative lifetime by Hupfield,<sup>39</sup> who used an instrument employing Kerr-cell optical shutters to measure directly the time decay of the fluorescence. He investigated the molecules Na<sub>2</sub>, K<sub>2</sub>, and I<sub>2</sub> and found them all to have the same lifetime, about 1×10<sup>-8</sup> sec. More recent work<sup>40</sup> on I<sub>2</sub>, for example, has shown that Hupfield's measurements are not reliable and must be regarded as more qualitative than quantitative.

However, we are in a position to determine the radiative lifetime of the (v'=10, J'=12) level of the Na<sub>2</sub> B <sup>1</sup>Π<sub>u</sub> state from the experimentally determined gτ product if we use a theoretical estimate for the value of the molecular g factor. In the case under study we have found that the variation of P(H) with H is Lorentzian to within the precision of our measurements. From this we conclude that the coupling scheme does not change with applied field. Moreover, we have found that the degree of polarization P(0) at zero field is the same (to better than 1%) as the value calculated ignoring hyperfine structure. Thus we are led also to conclude that Fig. 6(a) describes the coupling of the (v'=10, J'=12) level of the Na<sub>2</sub> B <sup>1</sup>Π<sub>u</sub> state for all magnetic-field strengths.

This latter conclusion may seem at first surprising since it might be expected that in the absence of external fields **J** and **T** must couple together. Then at zero-magnetic field it seems paradoxical to obtain experimentally the degree of polarization appropriate to the uncoupled case. However, the hyperfine effects discussed in Part A and B of this section all *assume that T and J precess rapidly about the resultant F compared to the radiative lifetime*. If the hyperfine interaction is

weak, though, this will no longer be true and we may say that the excited state does not live long enough for the hyperfine coupling to have any effect. We believe that this is the case for the (v'=10, J'=12) level of the Na<sub>2</sub> B <sup>1</sup>Π<sub>u</sub> state and accounts for the behavior we have observed. A similar situation in the case of atomic excited states has been discussed by Lehmann.<sup>41</sup> Note that this has the important general consequence that whenever the hyperfine interaction splittings are much less than the natural width of the excited state, the level-crossing signal will be little altered by considerations based on the hyperfine coupling.

Based on the angular momentum coupling model shown in Fig. 6(a) the molecular g factor is calculated to be g<sub>J</sub> = 0.00641 ± 3%. We have included a 3% uncertainty in this theoretical value to allow for all other possible hyperfine splittings, perturbations, etc., which might cause the molecular g factor to deviate from the value we have calculated. Using this g value and the experimentally determined gτ product, the radiative lifetime of the (v'=10, J'=12) level of the B <sup>1</sup>Π<sub>u</sub> Na<sub>2</sub> molecule is calculated to be τ = 6.41 ± 0.38 × 10<sup>-9</sup> sec. This molecular lifetime is more than a factor of two shorter than the lifetime of the (atomic) sodium D lines,<sup>42</sup> τ<sub>Na D</sub> = 16.1 ± 0.3 × 10<sup>-9</sup> sec, and represents one of the fastest molecular transitions yet measured in the visible part of the spectrum.

### ACKNOWLEDGMENTS

We would like to thank Dr. Harold S. Boyne, Chief of Division 271, National Bureau of Standards, and Dr. Lewis M. Branscomb, Chairman of the Joint Institute for Laboratory Astrophysics, whose support and encouragement made this collaborative venture possible.

<sup>39</sup> H. H. Hupfield, Z. Physik **54**, 484 (1929).

<sup>40</sup> R. A. Berg, thesis, University of California, Lawrence Radiation Laboratory Report UCRL-9954 March, 1962; L. Brewer, R. A. Berg, and G. M. Rosenblatt, J. Chem. Phys. **38**, 1381 (1963).

<sup>41</sup> J. C. Lehmann, J. Phys. Radium **25**, 809 (1964). We thank Dr. Peter L. Bender of the Joint Institute for Laboratory Astrophysics, Boulder, Colo., for pointing out this reference to us.

<sup>42</sup> J. K. Link, J. Opt. Soc. Am. **56**, 1195 (1966).